Crystal Structure of Syndiotactic Polypropylene

Claudio De Rosa* and Paolo Corradini

Dipartimento di Chimica, Università di Napoli Federico II, Via Mezzocannone 4, 80134 Napoli, Italy

Received February 16, 1993; Revised Manuscript Received May 12, 1993

ABSTRACT: An analysis of the crystal structure on unoriented and oriented samples of syndiotactic polypropylene is presented, on the basis of a comparison between calculated structure factors and experimental X-ray diffraction intensities. According to the present analysis, syndiotactic polypropylene can exist in different orthorhombic modifications having chains in helical conformation. Stretched samples may contain, at least in part, the *C*-centered structure proposed by Corradini et al. (limit space group $C222_1$), while single crystals and polycrystalline samples are generally in the structure proposed by Lotz, Lovinger, Cais, and Davis (limit space group *Ibca*). Calculations of structure factors indicate that the two polymorphic forms of s-PP may be characterized by various degrees of disorder depending on the chemical and physical history of the sample. A possible disorder present is related to the statistical substitution of right and left handed helices along the same lattice axes. The space groups for the two limit statistical structures are *Cmcm* and *Bmcm*.

Introduction

The polymorphic behavior of syndiotactic polypropylene (s-PP) has been well-known for many years.[1-3] Different crystalline modifications of s-PP having helical chain conformation[3] as well as one having a zigzag planar chain conformation have been described.[2,4,5]

The crystal structure of a polymorph of s-PP was reported, for the first time, by Corradini et al. in 1967.[3] Chains in helical conformations $(TTGG)_2$ (s(2/1)2 symmetry) are packed in an orthorhombic unit cell with axes $a = 14.50$ Å, $b = 5.60$ Å, and $c = 7.40$ Å, the proposed space group for the most ordered crystalline portions being $C222_1$.[3]

This structure is characterized by a centering of the *ab* face of the unit cell (*C*-centered structure with chain axes in $(0, 0, z)$ and $(1/2, 1/2, z)$) (Figure 1A). The structure was deduced from the X-ray diffraction spectra of drawn fibers of s-PP samples then available.[3]

Recently Lotz, Lovinger and Cais[6] succeeded in growing highly regular single crystals of s-PP and performed the first electron diffraction analysis on single crystals of this polymer. They found the same molecular conformation and basic unit cell dimensions but a different interchain packing as Corradini et al. did.[3] The space group proposed by the authors in ref 6 is $Pca2_1$, it could be taken as *Pcaa* if the full symmetry of the chains is maintained in the lattice. This structure is characterized by an antichiral packing along the *a* axis, that is by the presence of helices of opposite hand with chain axes in $(0, 0, z)$ and $(1/2, 0, z)$ (Figure 1B). Moreover they have tentatively proposed the possibility that the true unit cell may be more complex, i.e. doubled along the *b* axis. In this model the chains alternate in hand also along the *b* axis (Figure 1C); the space group proposed is *Ibca*.[6]

The presence in literature of two different models of packing of the chains of s-PP arises from different experimental observations. In fact the model of Figure 1A was based on the observation, in the X-ray fiber diffraction spectrum,[3] of a reflection at $2\theta = 17°$ ($d = 5.22$ Å), indexed with the traditional unit cell as 110; the models of Figure 1B,C were instead based on the observation, in the electron diffraction spectra, of single crystals,[6] of a reflection at $2\theta = 15.9°$ ($d = 5.57$ Å) indexed as 010.

Lovinger, Lotz, and Davis[7] have then demonstrated the generality of a possible mode of packing with chain axes in $(0, 0, z)$ and $(1/2, 0, z)$ (Figure 1B) not only for single crystals in ultrathin films, but also for polycrystalline thick films, for bulk specimens obtained directly from the polymerization, and for oriented thin films. Finally they have studied the dependence of the s-PP molecular packing with the temperature of crystallization of single crystals.[8] In particular they have found that at low temperatures of growth (<80 °C), disorder in the packing of *bc* layers of macromolecules is progressively introduced. The disorder consists in the statistical occurrence of the juxtaposition of layers locally packed between themselves as in the *C*-centered structure of the kind proposed by Corradini et al.,[3] with chain axes in $(0, 0, z)$ and $(1/2, 1/2, z)$.

According to the idea of Lovinger, Lotz, and Davis[7,8] the *C*-centered structure exists only as a defect structure

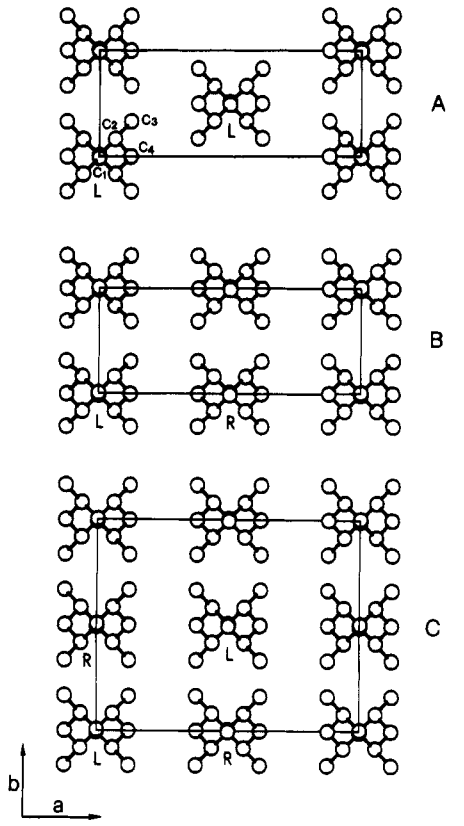

Figure 1. Model of packing of limit orthorhombic modifications of s-PP: (A) space group $C222_1$; (B) space group *Pcaa*; (C) space group *Ibca*. R = right handed helix; L = left handed helix.

0024-9297/93/2226-5711$04.00/0 © 1993 American Chemical Society

in their prevailing packing and, in fact, at no growth temperature they have observed a regular *C*-centered packing.

More recently Lovinger, Lotz, and Davis[9] have repeated the electron and X-ray diffraction investigation of the structure of s-PP due to the availability of a new highly syndiotactic sample synthesized with the new Ziegler–Natta homogeneous catalysts described by Ewen et al.[10]

From this study the authors conclude that in single crystals of highly syndiotactic polypropylene the preferred packing mode is that of Figure 1C, i.e. with the unit cell having a doubled *b* axis ($b = 11.2$ Å), in which the molecules alternate in hand along both the *a* and *b* axes.

This conclusion arises from the clear observation, in the electron diffraction of single crystals isothermally crystallized at high temperature (e.g. 140 °C), of a strong, discrete reflection at $2\theta = 18.9°$ ($d = 4.70$ Å) and indexed with the cell having $b = 11.2$ Å as the 211 reflection.[9] Moreover Lovinger, Lotz, and Davis[9] observe, in their electron and X-ray diffraction spectra, the absence of the reflection at $2\theta = 16.95°$ ($d = 5.22$ Å), indexed as 110 reflection with the cells of Figure 1A,B. This reflection is permitted only by the original *C*-centered cell of Figure 1A; therefore, the authors conclude that this mode of packing is inconsistent with the experimental evidence. The 110 reflection ($d = 5.22$ Å) was instead observed in the previous less stereoregular samples[6-8] in which the presence of isotactic sequences, which were sufficiently long so as to crystallize, was revealed by the presence of reflections at $2\theta = 14.1$ and 18.6° typical of isotactic polypropylene. For this reason Lovinger, Lotz, and Davis[9] make the observation that the reflection at $2\theta = 16.95°$ ($d = 5.22$ Å) may arise not from s-PP but from its isotactic admixture for which the strong 040 reflection would occur at the same observed spacing. They conclude, finally, that the absence of this peak in their new spectra confirms their original interpretation and validates their alternative packing scheme (cells in Figure 1B,C), while the *C*-centered packing model (Figure 1A) was definitively ruled out.

It is worthy to note that, although all the work of Lovinger, Lotz, Cais, and Davis[6-9] has given an important contribution to clarify the polymorphism of s-PP, analyses on oriented fiber specimens have never been reported. On the other hand it is well-known that the occurrence of a transition between different crystalline forms under tensile stress is often associated with the change of the morphology.[11] We recall, for instance, the solid-to-solid transitions under stress of nylon 6,[12] poly(vinylidene fluoride),[13,14] poly(butylene terephthalate),[15-19] and syndiotactic poly(1-butene).[20]

In this paper an analysis of the crystal structure on unoriented and oriented samples of s-PP is presented, in order to show that the two models of packing of s-PP (Figure 1A and Figure 1B,C) are not alternative models (i.e. they do not correspond to different interpretations of one single type of crystal), but they represent two different limiting models of the structure of s-PP. The two models correspond to substantially different crystals, with different X-ray diffraction patterns, even if mixed, in samples of different morphology. In particular we will show that in fiber specimens a mixture of the two different modifications, corresponding to the models of Figure 1A and Figure 1B,C, occurs and that the reflection at $2\theta = 16.95°$ should be attributed to s-PP.

Calculations of structure factors, performed for the various proposed models of packing, are presented in comparison with our X-ray diffraction data and with electron diffraction data reported in the literature.[6-9]

Our X-ray diffraction characterizations are performed on s-PP samples synthesized with the new Ziegler–Natta homogeneous catalysts, described for the first time by Ewen et al.[10] These samples of s-PP have high degrees of syndiotacticity and crystallinity quite similar to those of the sample used in ref 9, and do not present any traces of isotactic crystallinity.

Experimental Section

The s-PP was supplied by "Himont Italia". The polymer was synthesized with syndiospecific homogeneous catalyst based on the column 4 (group 4A) metallocene/methylalumoxane system.[10] Two different samples were studied: sample A ($MW = 260 \times 10^3$) and sample B ($MW = 120 \times 10^3$), obtained by performing the polymerization at 0 and 44 °C respectively. (These samples correspond to samples 1 and 5 of ref 21.) The materials are highly syndiotactic; in fact, the fully syndiotactic pentads are 94.5% and 88.6% for samples A and B respectively.

Slow crystallizations from the melt of samples A and B were performed by heating the samples up to ≈200 °C under a press and successive cooling to room temperature at a cooling rate of 1.5 °C/min (compression-molded samples).

Oriented samples were obtained by drawing at room temperature (draw ratio ≈ 6; draw rate ≈ 5 mm/min) the compression-molded samples A and B.

Wide angle X-ray diffraction spectra were obtained with nickel-filtered Cu Kα radiation. The diffraction patterns of unoriented samples were performed with an automatic Philips diffractometer. Those for oriented samples were obtained with a photographic cylindrical camera.

Observed structure factors (F_o) have been obtained as the square root of the experimental intensities corrected by $LP = (1 + \cos^2 2\theta)/(\sin^2 \theta \cos \theta)$, $F_o = (I/LP)^{1/2}$. The experimental intensities have been evaluated by measuring the area of the peaks in the X-ray powder diffraction patterns, after subtraction of the amorphous halo. The shape of the amorphous halo was taken from Figure 1a of ref 22.

Calculated structure factors (F_c) have been obtained as $F_c = (\sum |F_i|^2 M_i)^{1/2}$ where M_i is the multiplicity factor and the summation is taken over all the reflections included in the 2θ range of the corresponding reflection peak observed in the Geiger spectrum. It was assumed a thermal factors $B = 8$ Å^2 and the atomic scattering factors as in ref 23.

The indices of the reflections are given for the traditional unit cell with axes $a = 14.5$ Å, $b = b' = 5.60$ Å, $c = 7.40$ Å and for the unit cell for which *b* is doubled, $b = 2b' = 11.2$ Å. The notation used when indices are referred to the unit cell with $b = b'$ or $b = 2b'$ are *hkl* ($b = b'$) and *hkl* ($b = 2b'$), respectively.

Results and Discussion

Powder Samples. The X-ray powder diffraction patterns of the as-prepared samples A and B of s-PP are reported in Figures 2a and 3a respectively. In Figures 2b and 3b are reported the X-ray powder diffraction patterns of the compression-molded samples A and B respectively.

From these spectra, the high crystallinity (≈50%) and the absence of any traces of isotactic crystallinity in samples A and B are apparent.

It is worthy to note that the four spectra of Figures 2 and 3 show several differences indicating a changing crystalline structure of s-PP. In particular, for the as-prepared sample A, the spectrum of Figure 2a presents a diffraction peak at $2\theta = 15.9°$ ($d = 5.57$ Å), indexed as the 010 reflection with the unit cell with axes $a = 14.50$ Å, $b = 5.60$ Å, $c = 7.40$ Å, typical of a packing mode of the kind of Figure 1B. For sample A slowly crystallized from the melt, the ordered modification with packing mode of the chains of Figure 1C occurs, as is apparent from the presence, in the spectrum of Figure 2b, of the reflection at $2\theta = 18.9°$ ($d = 4.70$ Å) and indexed with the cell having the doubled *b* axis ($b = 11.2$ Å) as the 211 reflection. This confirms the results already reported in ref 9.

For the less stereoregular sample B, slow crystallization from the melt does not produce the ordered modification of Figure 1C, as is apparent from the absence, in the

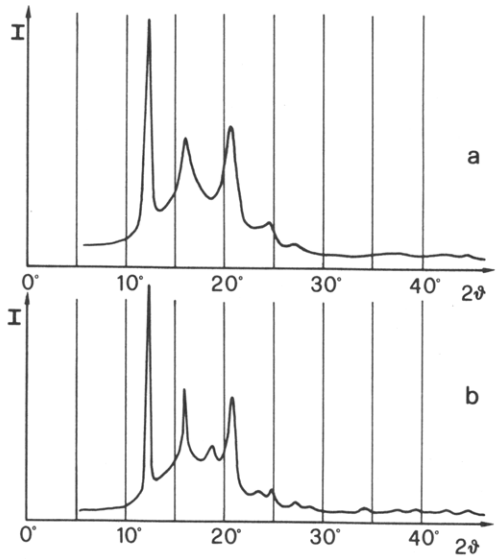

Figure 2. X-ray powder diffraction patterns of sample A of s-PP: (a) as-prepared sample; (b) compression-molded sample.

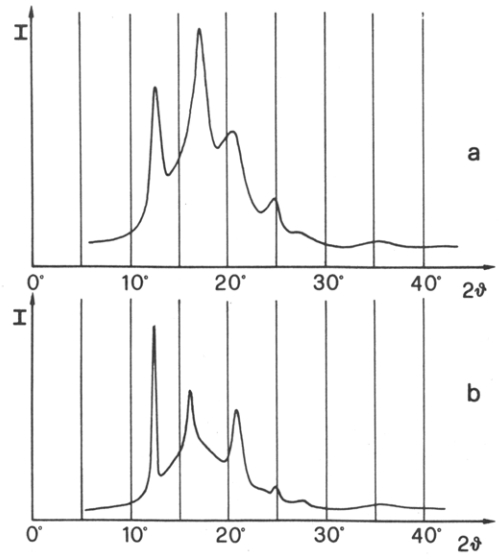

Figure 3. X-ray powder diffraction patterns of sample B of s-PP: (a) as-prepared sample; (b) compression-molded sample.

spectrum of Figure 3b, of the reflection at $2\theta = 18.9°$ ($d = 4.70$ Å); the packing mode of Figure 1B is instead prevalent as revealed by the presence of the 010 ($b = b'$) reflection at $2\theta = 15.9°$ ($d = 5.57$ Å).

The X-ray powder diffraction spectrum of the as-prepared sample B (Figure 3a), presents a large diffraction peak in the 2θ range 15–18° maximized at $2\theta = 17°$ ($d = 5.22$ Å) on the 110 ($b = b'$) reflection, typical of a packing mode of the kind seen in Figure 1A. Therefore, in the as-prepared sample B, we think that disorder in the stacking of layers of macromolecules *bc* is present, so that the long range crystal structure could be described by a (coherent) stacking of the limit ordered structures of Figure 1A,B.

This is in accordance with the observation by Lovinger, Davis, and Lotz[8,9] that the *h*10 ($b = b'$) reflections exhibit streaking in the electron diffraction spectra of single crystals grown isothermally at low temperature. Small but distinct diffuse maxima were seen in the position of the 110 ($b = b'$) reflection ($d = 5.22$ Å) although the resulting diffuse scattering remains maximized at the 010 ($b = b'$) reflection ($d = 5.57$ Å).[8,9] It appears that at lower growth temperatures the crystallographic register in the repetition along *a* is progressively lost.

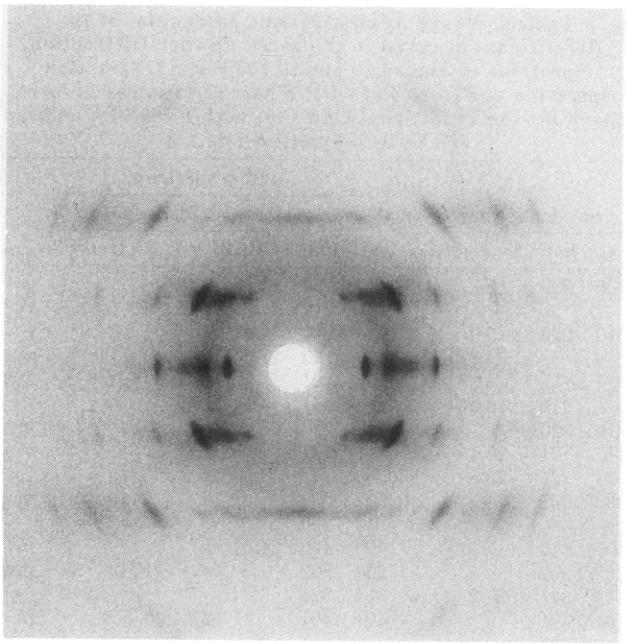

Figure 4. X-ray fiber photographic spectrum of oriented sample A of s-PP.

The presence of this polymorphism is also pointed out by the results of calculations of packing energy of chains of s-PP in a bidimensional and threedimensional lattice recently reported.[24] In fact it was shown that the two limit ordered structures, corresponding to the space groups $C222_1$ and *Pcaa*, have practically the same energy.[24] The stacking of layers of macromolecules having their axes in the *bc* plane do not have hard constraints, but for the interlayer distances (14.5/2 = 7.25 Å), long range order in the positioning of the methyl groups within each layer *bc* (but not the chirality of the macromolecules) seems to be always prescribed by the calculations[24] with a fixed distance between the axes of the macromolecules (5.6 Å).

Fiber Samples. Fibers of samples A and B, obtained by drawing at room temperature the compression-molded samples, show the X-ray diffraction fiber spectrum typical of the zigzag planar modification,[4] the 2-fold helix type structure being completely absent. The zigzag planar modification can be converted to the 2-fold helix type structure by annealing the fiber samples, holding the ends fixed to avoid the losing of orienation. This transition is complete in 30 min at 100 °C for fiber B and at 120 °C for fiber A.

The X-ray diffraction fiber photographic spectrum of the oriented sample A after annealing is reported in Figure 4 (the spectrum of the oriented sample B is very similar).

The Bragg angles and the intensities of the reflections observed in the X-ray fiber spectrum of Figure 4 are listed in Table I in comparison with those of the reflections observed in the powder spectrum of the compression-molded sample A of Figure 2b.

It is apparent from Figure 4 and Table I that in the fiber spectrum both the 010 ($b = b'$) (at $2\theta = 15.9°$, $d = 5.57$ Å) and 110 ($b = b'$) (at $2\theta = 17°$, $d = 5.22$ Å) reflections are present. Thus, for specimens prepared by annealing-induced solid-state transformation of oriented samples of the all-*trans* planar phase, with their ends kept clamped, we have the partial appearance of packing mode of the kind seen in Figure 1A. Therefore annealed fiber samples A, as well as annealed fiber samples B, prepared as described before, are characterized by a mixture of the limiting ordered structures of Figure 1A and Figure 1B or 1C.

Table I. Bragg Angles (2θ) and Intensities of the Reflections Observed in the X-ray Powder Diffraction Spectrum of Figure 2b and in the Fiber Diffraction Spectrum of Figure 4 of s-PP Where the Indices *hkl* Are Given for the Traditional Unit Cell with b = 5.60 Å and for the Unit Cell with b = 11.2 Å

powder spectrum				fiber spectrum						
						2θ, deg				
hkl[a]	hkl[b]	2θ, deg	I_{obs}	hkl[a]	hkl[b]	$l=0$	$l=1$	$l=2$	$l=3$	I_{obs}
200	200	12.2	vs	200	200	12.25				vs
					011		14.5			vw
010	020	15.9	s	010	020	15.9				s
		–		110	120	17.0				s
		–		201	201		17.1			mw
	211	18.9	m		211		18.9			w
210	220			210	220	20.0				mw
111	121	20.6	vs	111	121		20.7			vs
211	221	23.5	w							
002	002			002	002			24.0		ms
		24.5	mw	310	320					
400	400			400	400	24.5				ms
202	202			202	202			27.0		mw
311	321	27.2	mw	311	321					
401	401			401	401		27.4			m
	411									
012	022	28.9	vw	012	022			28.9		w
410	420			410	420	29.5				vvw
	231	29.5	vw							
112	122									
	312									
212	222	31.5	vw							
411	421									
312	322			312	322			34.4		ms
	132	34.5	w	220	240					
				510	520	34.5				vw
221	241			221	241					
511	521	37.0	vw	511	521		36.8			mw
412	422			412	422			38.3		vw
321	341	39.0	vw	321	341		39.6			vw
				420	440	41.0				vw
222	242			222	242					
512	522	42.6	w	512	522			42.6		m
				421	441		42.7			w
313	323			313	323					
322	342	44.6	w	403	403				44.0	w
602	602			602	602			45.0		vvw
					413					
					233				46.6	vw
612	622									
422	442	47.8	w	422	442			47.4		m
123	143			023	043				48.9	w
620	640	49.5	w	620	640					
				800	800	50.5				vvw
				223	243					
				513	523				50.5	vw
				132	162					
				622	642			56.1		vvw

[a] Indices *hkl* for the unit cell with b = 5.60 Å. [b] Indices *hkl* for the unit cell with b = 11.2 Å.

In conclusion the X-ray powder and fiber diffraction data clearly indicate the presence of different orthorhombic modifications having chains in 2-fold helix conformation; annealed fibers samples are partly in the C-centered structure proposed by Corradini et al.[3] (space group $C222_1$, Figure 1A), while specimens obtained under the most common conditions, powder, single crystals, etc., are prevailingly in the structure proposed by Lotz, Lovinger, Cais, and Davis[6-9] (space group *Pcaa*, Figure 1B, or *Ibca*, Figure 1C); sometimes, as in single crystals grown at high crystallization temperatures, the pure packing mode of Figure 1C is obtained.[9]

Calculations of Structure Factors. The calculations of structure factors have been performed for all the compatible space groups considered in the packing energy calculations reported in ref 24 ($C222_1$, *Pnan*, *Pbnn*, $I2_12_12_1$, *Pcaa*, *Pmna*, *B222*, *Pbcb*, *Ibca*, *Bbab*, *Cmca*, *Cmcm*, *Bmcm*), but only the more significant results are reported. The fractional coordinates of the asymmetric unit employed are those reported by Corradini et al.[3] and rewritten in Table II for all the space groups here considered.

A comparison between experimental intensities, observed in the X-ray fiber diffraction spectrum of Figure 4 and in the electron diffraction spectra reported in the literature,[6-9] and calculated structure factors, $F_c^2 = |F|^2 M$, for the models of Figure 1A (space group $C222_1$), Figure 1B (space group *Pcaa*) and Figure 1C (space group *Ibca*) is reported in Table III (notice that the indices of the reflections are given for the traditional unit cell with b = 5.60 Å, and for the unit cell for which b is doubled). It is worthwhile to note that the comparison between the experimental electron diffraction intensities and the calculated F_c^2 is given just as an indication because of the different atomic scattering factors employed in the calculations.

It is apparent that the electron diffraction data are accounted for by the space group *Ibca*. Some discrepancy is, however, still present for the space group *Ibca*; for instance the 011 ($b = 2b'$) reflection, observed in the electron diffraction spectrum of Figure 4a of ref 9, is not permitted by the space group *Ibca*; it could be explained by a mode of packing similar to that of Figure 1C (space group *Ibca*), but in a space group of lower symmetry.

Regarding fiber diffraction data, we recall that our fiber sample is characterized by a mixture of the two limit modifications of Figure 1A and Figure 1C. Therefore, the reflections arising from the diffraction of crystals of the modification of Figure 1A are indicated in Table III with an asterisk, while those arising from the diffraction of crystals of the modification of Figure 1C are indicated with two asterisks. The reflections without symbols are common to both the modifications.

It is apparent that the reflections indicated with an asterisk are accounted for by the space group $C222_1$ while those indicated with two asterisks are accounted for by the space group *Ibca*.

An analogous comparison, between observed structure factors, $F_o = (I/\mathrm{LP})^{1/2}$, obtained by experimental intensities taken from the X-ray powder diffraction patterns of Figure 2a,b, and calculated structure factors, for the models of Figure 1A–C, is reported in Table IV. As mentioned before, the X-ray powder diffraction data of Figure 2b are accounted for by the model of Figure 1C (space group *Ibca*).

The comparison between the space groups *Ibca* and *Pcaa* is interesting. As shown in Tables III and IV the best agreement between experimental intensities in the electron diffraction and in the X-ray powder diffraction spectrum of Figure 2b, and those calculated is obtained for the space group *Ibca*. In fact, first of all, the reflections 211 ($b = 2b'$), 411 ($b = 2b'$), and 231 ($b = 2b'$), observed in the electron diffraction spectra,[9] at spacings of d = 4.70, 3.13, and 3.03 Å, respectively (see Table III), are identifiable only with the cell with doubled b axis (Figure 1C). Moreover the 201 and 221 ($b = 2b'$) reflections, at calculated spacings d = 5.179 and 3.802 Å, respectively, are absent or have weak intensities in the X-ray powder and electron diffraction spectra. While their calculated intensities are high for the space group *Pcaa*, they are extinct for the space group *Ibca* (see Tables III and IV). As a matter of fact, the low observed intensity of the 211 ($b = 2b'$) reflection (d = 4.70 Å) with respect to the calculated one for the space group *Ibca* (Table IV) and the presence of the 221 ($b = 2b'$) reflection (d_{obs} = 3.79 Å), although of weak intensity, in the powder spectrum of Figure 2b (Table IV), could indicate the presence in the crystals of a small

Table II. Fractional Coordinates of the Asymmetric Unit of s-PP for the Space Groups $C222_1$, *Cmcm*, *Pcaa*, *Bmcm*, and *Ibca*[a]

	$C222_1$, *Cmcm*			*Pcaa*, *Bmcm*			*Ibca*		
	x/a	y/b	z/c	x/a	y/b	z/c	x/a	y/b	z/c
C_1	0.000	0.010	0.250	0.250	0.010	0.000	0.250	0.0050	0.000
C_2	0.061	0.165	0.385	0.311	0.165	0.135	0.311	0.0825	0.135
C_3	0.122	0.331	0.241	0.372	0.311	0.991	0.372	0.1655	0.991
C_4	0.121	0.000	0.500	0.371	0.000	0.250	0.371	0.0000	0.250

[a] The asymmetric unit corresponds to the atoms labelled in Figure 1. For the space group *Ibca* the fractional coordinates are calculated for the unit cell with $b = 11.2$ Å.

fraction of local structures corresponding to the ideal model of Figure 1B (space group *Pcaa*).

These conclusions arise from the comparison between the calculated intensities and the X-ray powder diffraction spectrum of Figure 2b; it is apparent that for the other powder spectrum, e.g., that of Figure 2a or 3b, in which the 211 ($b = 2b'$) reflection at $d = 4.70$ Å seems to be absent, the best agreement would be obtained for the space *Pcaa* or for models in which some type of disorder occurs, as will be discussed in the following section.

Disorder in the Structure. It is worthwhile to note that in all the experimental data reported (X-ray powder and fiber diffraction data and electron diffraction data) the absence or the weak intensity of some reflections seems to show the occurrence of statistical disorder in the structures. For the modification of Figure 1A, occurring partly in annealed fiber samples, it is apparent, from Figure 4 and the data of Table III, that the 201 ($d = 5.18$ Å) and 401 ($d = 3.26$ Å) reflections have weak or medium intensities in the fiber spectrum while their calculated intensities, for the space group $C222_1$, are high; in particular, the diffuse scattering along the first layer line surrounding the position of the 201 reflection, observed in the fiber spectrum of Figure 4, indicates the presence of disorder. Moreover in the electron diffraction spectra of single crystals crystallized at low temperature,[8,9] the strong 211 ($b = 2b'$) reflection at $d = 4.70$ Å is replaced by diffuse streaks along $h11$, indicating the occurrence of disorder in regions of real crystals, having a structure corresponding to the ideal type of Figure 1C.

As regards the powder samples, the X-ray diffraction spectra, reported in Figures 2 and 3, show that only sample A, slowly crystallized from the melt, presents a discrete 211 ($b = 2b'$) reflection peak at $d = 4.70$ Å (Figure 2b) indicating the presence of the ordered modification of Figure 1C (space group *Ibca*). The other spectra of Figures 2a and 3a,b are not accounted for by the space group *Ibca* or by the space group *Pcaa* (model of Figure 1B). In fact the absence of the 211 ($b = 2b'$) reflection at $d = 4.70$ Å allows us to discard the space group *Ibca*. Moreover, the calculated intensities, for the space group *Pcaa*, of the 201 and 221 ($b = 2b'$) reflections at calculated spacings $d = 5.179$ Å and $d = 3.802$ Å, respectively, are high; these reflections are absent or have very weak intensity in the spectra of Figures 2a and 3a,b. It is worthwhile to note that the 221 ($b = 2b'$) reflection (at $2\theta = 23.5°$) is present in the spectrum of Figure 2b, although of weak intensity, but it is absent in the spectra of Figures 2a and 3a,b. Disorder has to be invoked to explain these spectra.

For the polymorph of Figure 1B,C a possible disorder present could be related to the statistical substitution of right- and left-handed helices about each axis (0, 0, z) and ($^1/_2$, 0, z) of the unit cell, giving rise to a statistical departure from regular fully antichiral packing along both axes. The space group for the limit statistical structure would be *Bmcm*. For the polymorph of Figure 1A the statistical substitution of right and left handed helices about each axis (0, 0, z) and ($^1/_2$, $^1/_2$, z) of the unit cell produces the statistical space group *Cmcm*. Calculated structure factors for the space groups *Bmcm* and *Cmcm* are also reported in Tables III and IV. In Table IV the calculated intensities are compared also with the observed structure factors F_o obtained by experimental intensities taken from the X-ray powder diffraction pattern of Figure 2a.

It is apparent that some degree of disorder has to be invoked for both the polymorphs of Figure 1A and Figure 1B,C. In fact from Table III, it is apparent that the space group *Cmcm* implies the systematic absence of the 201 and 401 reflections; therefore models where the local correlation about the chirality of neighboring chains is preserved can be accounted for by the incomplete absence of the reflections in question.

From Table IV, it is apparent that the space group *Bmcm* gives a fairly good agreement only for the experimental intensities taken from the spectrum of Figure 2a. Also in this case, however, models where local correlation about the chirality of neighboring chains is preserved seem to be more suitable.

Conclusions

Syndiotactic polypropylene can exist in different orthorhombic modifications having chains in helical conformation.

Annealed fiber samples are partly in the C-centered structure proposed by Corradini et al.[3] (Figure 1A), while specimens obtained under the most common conditions, powder, single crystals, etc., are prevailingly in the structure proposed by Lotz, Lovinger, Cais, and Davis[6-9] (Figure 1B,C); sometimes, as in single crystals grown at high crystallization temperatures, the pure packing mode of Figure 1C is obtained.[9] Mixture of these modifications can be obtained in disordered samples.

The first modification (Figure 1A) is characterized by the packing of helices with chain axes in the position (0, 0, z) and ($^1/_2$, $^1/_2$, 0) of the unit cell, neighboring helices being prevailingly of the same hand. The space group proposed for this ordered limit structure is $C222_1$.[3]

The second modification (Figure 1B,C) is characterized by the packing of helices with chain axes in (0, 0, z) and ($^1/_2$, 0, z), neighboring helices being prevailingly of the opposite hand. The space group corresponding to the limit structure of Figure 1B is *Pcaa*.[6] Fully antichiral packing along both axes, involving a unit cell with doubled b axis (Figure 1C), occurs for highly ordered samples. The space group corresponding to this limit structure, is *Ibca*.[6]

Space groups $C222_1$, for the first form, and *Ibca*, for the second one, correspond to limit-ordered modifications. Both the polymorphic forms of Figure 1A and Figure 1B,C are instead characterized by the presence of some degree of disorder in the structures, as is apparent from the calculations of structure factors. A possible disorder present could be related to the statistical substitution of right- and left-handed helices in the corresponding lattice positions. The space groups for the limit statistical structures are *Cmcm*, for the modification of Figure 1A and *Bmcm* for that of Figure 1B,C.

It is worthy to note that these space groups represent a condition of statistical disorder in which it is not possible

Table III. Comparison between Experimental Intensities, I_{obs}, Observed in the X-ray Diffraction Fiber Spectrum of Figure 4 and in the Electron Diffraction Spectrum Reported in the Literature,[6-9] and Calculated Structure Factors, F_c^2, for the Space Groups $C222_1$, *Pcaa*, *Ibca*, *Cmcm*, and *Bmcm* Where the Indices Are Given for the Traditional Unit Cell Having b = 5.60 Å and for the Unit Cell for Which b Is Doubled

					F_c^2						
	hkl^a	hkl^b	d_{obs}[c]	d_{calc}	$C222_1$	*Pcaa*	*Ibca*	*Cmcm*	*Bmcm*	I_{obs}[d]	I_{obs}[e]
	200	200	7.23	7.250	300	300	300	300	300	vs	vs
**	010	020	5.57	5.600	...	160	160	...	160	s	s
*	110	120	5.22	5.224	290	...	...	290	...	s	...
**	210	220	4.44	4.432	...	190	190	...	190	mw	ms
	310	320		3.659	97	...	...	97	...		...
			3.63		185	88	88	185	88	ms	
	400	400		3.625	88	88	88	88	88		m
**	410	420	3.03	3.043	...	36	36	...	36	vvw	w
	220	240		2.612	2	2	2	2	2		
*			2.60		11	2	2	11	2	vw	
	510	520		2.575	9	...	...	9	...		
	420	440	2.20	2.216	15	15	15	15	15	vw	
	030	060		1.867	...	15	15	...	15	...	
	130	160		1.851	13	...	...	13	...	...	
	620	640		1.830	19	19	19	19	19		
			1.81		32	32	32	32	32	vvw	
	800	800		1.813	13	13	13	13	13		
		011	6.09	6.174	...	...	...	...	...	vw	vvw
*	201	201	5.18	5.179	140	140	...	...	...	mw	...
**		211	4.70	4.701	...	...	230	...	...	w	s
	111	121	4.29	4.268	400	350	350	350	350	vs	vs
	211	221		3.802	...	130	...	...	...	...	...
	311	321		3.280	110	16	16	16	16		w
*			3.26		161	67	16	16	16	m	
	401	401		3.255	51	51	...	...	...		...
		411		3.126	...	...	73	...	...	–	w
		231		3.029	...	...	45	...	...	–	w
	411	421		2.814	...	22	...	...	...	...	...
	221	241		2.463	23	6	...	16	...		...
			2.44		78	61	55	71	55	mw	
	511	521		2.432	55	55	55	55	55		
**	321	341	2.28	2.303	...	50	50	...	50	vw	
	611	621		2.125	...	3	...	...	...	...	
*	421	441	2.12	2.123	49	5	...	45	...	w	
		631		1.957	...	...	11	...	...	–	
	521	541		1.944	...	10	10	...	10	–	
		451		1.845	...	...	11	...	...	–	
	621	641		1.776	17	16	...	1	...	...	
	002	002	3.70	3.700	75	75	75	75	75	ms	ms
	202	202	3.30	3.296	15	15	15	15	15	mw	
**	012	022	3.09	3.087	...	22	22	...	22	w	w
	112	122		3.019	19	9	...	10	...	...	
		312		2.842	...	...	17	...	...	–	
	212	222		2.840	...	20	20	...	20	...	w
*	312	322	2.61	2.602	170	48	...	120	...	ms	
		132		2.586	–	–	13	–	–	–	
**	412	422	2.35	2.350	...	160	160	...	160	vw	ms
		332		2.309	...	...	55	...	...	–	
		512		2.237	...	...	17	...	...	–	
	022	042		2.233	7	7	7	7	7	...	
	122	142		2.207	...	9	...	...	...	...	
	222	242		2.134	38	13	13	13	13		
*			2.12		158	51	13	98	13	m	
	512	522		2.114	120	38	...	85	...		
	322	342		2.027	...	32	...	...	...	–	
	602	602	2.02	2.023	6	6	6	6	6	vvw	
		532		1.947	...	...	33	...	...	–	
	612	622		1.903	...	15	15	...	15	...	
	422	442	1.91	1.901	100	77	77	77	77	m	m
	522	542		1.769	...	14	...	...	...	...	
	132	162		1.656	17	...	...	17	...		
*			1.64		29	6	6	29	6	vvw	
	622	642		1.640	12	6	6	6	6		
	802	802		1.628	11	11	11	11	11	...	
	313	323		2.045	30	30	30	30	30		
			2.05		36	36	30	30	30	w	
	403	403		2.039	6	6	...	...	...		
		413		2.006	...	...	7	...	...		
**			1.95				11			vw	
		233		1.980	...	...	4	...	...		
*	023	043	1.86	1.851	34	...	...	34	...	w	
	123	143		1.836	...	43	43	...	43	...	
	223	243		1.793	16	9	...	7	...		
*			1.80		27	13	4	11	4	vw	
	513	523		1.781	11	4	4	4	4		

[a] Indices *hkl* for the traditional unit cell with b = 5.60 Å. [b] Indices *hkl* for the unit cell with b = 11.2 Å. [c] Spacings (Å) observed in the X-ray fiber diffraction spectrum. [d] Intensities observed in the X-ray fiber diffraction spectrum. [e] Intensities observed in the electron diffraction spectrum reported in literature.[6,9] Key: vs = very strong, s = strong, ms = medium strong, m = medium, mw = medium weak, w = weak, vw = very weak, vvw = very very weak.

Table IV. Comparison between Observed Structure Factors, F_o (from the X-ray Powder Diffraction Spectra of Figure 2a,b), and Those Calculated, F_c, for the Space Groups $C222_1$, *Pcaa*, *Ibca*, and *Bmcm* Where the Indices Are Given for the Traditional Unit Cell Having b = 5.60 Å and for the Unit Cell for Which b Is Doubled

						$F_c = (\sum\|F_i\|^2 M_i)^{1/2}$			
hkl[a]	*hkl*[b]	d_{obs}[c]	d_{calc}	F_o[d]	F_o[e]	$C222_1$	*Pcaa*	*Ibca*	*Bmcm*
200	200	7.25	7.250	77	77	77	77	77	77
010	020	5.57	5.600	53	66	...	57	57	57
110	120	...	5.224	...	...	76	...	...	...
201	201	...	5.179	...	...	74	74	...	...
	211	4.70	4.701	48	...	...	...	96	...
210	220		4.432			...	62	62	62
		4.31		121	128	127	117	117	117
111	121		4.268						
211	221	3.79	3.802	28	...	...	72	...	...
002	002		3.700			39	39	39	39
310	320	3.64	3.659	47	50	44	...	...	...
400	400		3.625			42	42	42	42
202	202		3.296			24	24	24	24
311	321	3.28	3.280	30	32	65	25	25	25
401	401		3.255			45	45	...	...
	411		3.126			...	...	54	...
		3.09		25	22				
012	022		3.087			...	29	29	29
410	420		3.043			...	27	27	27
	231	3.03	3.029	24	22	...	...	42	...
112	122		3.019			27	19	...	...
	312		2.842			...	...	26	...
212	222	2.84	2.840	26	(18)[f]	...	28	28	28
411	421		2.814			...	30	...	...
312	322		2.602			82	44	...	...
	132	2.60	2.586	32	25	...	...	23	...
510	520		2.575			13	...	...	...
221	241		2.463			30	16	...	...
		2.43		33	40				
511	521		2.432			47	47	47	47
412	422		2.350			...	79	79	79
203	203	2.31	2.335	44	40	10	...	...	...
321	341		2.303			...	45	45	45
	512		2.236	(23)[f]	(23)[f]	...	...	26	...
022	042		2.233	(23)[f]	(23)[f]	16	16	16	16
420	440		2.216	(23)[f]	(23)[f]	17	17	17	17
122	142		2.207	(23)[f]	(23)[f]	...	19	...	...
222	242		2.134			39	23	23	23
611	621		2.125			...	11	...	...
421	441	2.12	2.123	35	30	44	14	...	...
512	522		2.114			70	39	...	...
313	323		2.045			35	35	35	35
403	403		2.039			15	15	...	...
322	342	2.03	2.027	36	35	...	36	...	...
602	602		2.023			16	16	16	16
	413		2.006	(24)[f]	(24)[f]	...	...	17	...
	233		1.980	(25)[f]	(25)[f]	...	...	13	...
	631		1.957	(27)[f]	(27)[f]	...	...	21	...
	532		1.947	(27)[f]	(27)[f]	...	...	36	...
521	541		1.944	(27)[f]	(27)[f]	...	20	20	20
612	622		1.903			...	25	25	25
422	442	1.90	1.901	40	37	64	56	56	56
030	060		1.867			...	17	17	17
130	160		1.851			16	...	...	...
023	043		1.851			37	...	...	...
	451	1.84	1.845	37	20	...	...	20	...
123	143		1.836			...	41	41	41
620	640		1.830			19	19	19	19

[a] Indices *hkl* for the unit cell with b = 5.60 Å. [b] Indices *hkl* for the unit cell with b = 11.2 Å. [c] Spacings (Å) observed in the X-ray powder diffraction spectrum of Figure 2b. [d] Observed structure factors from the spectrum of Figure 2b. [e] Observed structure factors from the spectrum of Figure 2a. [f] Reflections not observed in the Geiger spectra. The numbers in parentheses represent values of F_o corresponding to threshold intensities, taken as equal to half of the minimum observed.

to make a prediction about the chirality of two macromolecules separated by any long range vector. It is reasonable to suppose, however, that first neighboring macromolecules are correlated as far as the chirality.

The statistical substitution of left and right handed helices along the same axis is in accordance with the results of energetic calculations,[24] which show an identical outside envelope of right-handed (TTG^+G^+) and left-handed (G^-G^-TT) helices of s-PP in the s(2/1)2 symmetry, which corresponds to a nearly identical positioning of the methyl groups. On the other hand the presence of small amount of configurational defects of the kind ..*rrrmrrr*...[25] included in the crystal of s-PP allows us to suppose that an inversion of the chirality of the helix could achieved on this defect inside the crystal with a low cost of energy.

Besides the disorder in the positioning of right- and left-handed helices, another kind of disorder can be present, for instance in single crystals of s-PP crystallized at low temperatures[8,9] or in powder samples such as that of Figure 3a. In fact these single crystals show, in the

electron diffraction spectra,[8,9] streaking of the $h10$ ($b = b'$) reflections along the h direction of the reciprocal lattice, while the powder sample of Figure 3a show a large diffraction peak in the range 15–18°. This could be related to the presence of disorder in the stacking, along the a axis, of bc layers of macromolecules, so that the structure could be described by a mixture of the limit-ordered modifications of Figure 1A,B.

The problem of the occurrence of various kind of disorder in the crystalline lattice of s-PP and its effect on the X-ray diffraction spectra deserves a thorough examination. This subject and the relation with configurational defects included in the crystal will be discussed in detail in our subsequent paper.[26]

Acknowledgment. We thank Dr. E. Albizzati and Dr. M. Galimberti of Himont Italia for supplying the s-PP samples. Financial support from the Ministero dell'Università e della Ricerca Scientifica e Tecnologica and from the Progetto Finalizzato Chimica Fine e Secondaria del CNR is gratefully acknowledged.

References and Notes

(1) Natta, G.; Pasquon, I.; Corradini, P.; Peraldo, M.; Zambelli, A. *Atti Accad. Naz. Lincei, Cl. Sci. Fis., Mat. Nat., Rend.* **1960**, *28*, 539.
(2) Natta, G.; Peraldo, M.; Allegra, A. *Makromol. Chem.* **1964**, *75*, 215.
(3) Corradini, P.; Natta, G.; Ganis, P.; Temussi, P. A. *J. Polym. Sci., Part C* **1967**, *16*, 2477.
(4) Chatani, Y.; Maruyama, H.; Noguchi, K.; Asanuma, T.; Shiomura, T. *J. Polym. Sci., Part C* **1990**, *28*, 393.
(5) Pirozzi, B.; Napolitano, R. *Eur. Polym. J.* **1992**, *28*, 703.
(6) Lotz, B.; Lovinger, A. J.; Cais, R. E. *Macromolecules* **1988**, *21*, 2375.
(7) Lovinger, A. J.; Lotz, B.; Davis, D. D. *Polymer* **1990**, *31*, 2253.
(8) Lovinger, A. J.; Davis, D. D.; Lotz, B. *Macromolecules* **1991**, *24*, 552.
(9) Lovinger, A. J.; Lotz, B.; Davis, D. D. *Polym. Prepr.* **1992**, *33*, 270.
(10) Ewen, A. J.; Jones, R. L.; Razavi, A.; Ferrara, J. D. *J. Am. Chem. Soc.* **1988**, *110*, 6255.
(11) Corradini, P.; Guerra, G. *Adv. Polym. Sci.* **1992**, *100*, 183.
(12) Miyasaka, K.; Ishikawa, K. *J. Polym. Sci., Part A2* **1968**, *6*, 1317.
(13) Lando, J. B.; Olf, H. G.; Peterlin, A. *J. Polym. Sci., Part A* **1966**, *4*, 941.
(14) Hasegawa, R.; Takahashi, Y.; Chatani, Y.; Tadokoro, H. *Polym. J.* **1972**, *3*, 600.
(15) Jakeways, R.; Ward, I. M.; Wilding, M. A.; Hall, I. H.; Desborough, I. J.; Pass, M. G. *J. Polym. Sci., Polym. Phys. Ed.* **1975**, *13*, 799.
(16) Yokouchi, M.; Sakakibara, Y.; Chatani, Y.; Tadokoro, H.; Tanaka, T.; Yoda, K. *Macromolecules* **1976**, *9*, 266.
(17) Jakeways, R.; Smith, T.; Ward, I. M.; Wilding, M. A. *J. Polym. Sci., Polym. Lett. Ed.* **1976**, *14*, 41.
(18) Ward, I. M.; Wilding, M. A. *Polymer* **1977**, *18*, 327.
(19) Tashiro, K.; Nakai, J.; Kobayashi, M.; Tadokoro, H. *Macromolecules* **1980**, *13*, 137.
(20) De Rosa, C.; Venditto, V.; Guerra, G.; Pirozzi, B.; Corradini, P. *Macromolecules* **1991**, *24*, 5645.
(21) Balbontin, G.; Dainelli, D.; Galimberti, M.; Paganetto, G. *Makromol. Chem.* **1992**, *193*, 693.
(22) Natta, G.; Corradini, P.; Cesari, M. *Atti Accad. Naz. Lincei, Cl. Sci. Fis., Mat. Nat., Rend.* **1957**, *22*, 11.
(23) Cromer, D. J.; Maan, J. B. *Acta Crystallogr.* **1968**, *A24*, 321.
(24) Corradini, P.; Pirozzi, B.; Napolitano, R. *Atti Accad. Naz. Lincei, Cl. Sci. Fis., Mat. Nat., Rend.* **1991**, *2*, 341.
(25) Ammendola, P.; Shijing, X.; Grassi, A.; Zambelli, A. *Gazz. Chim. Ital.* **1988**, *118*, 769.
(26) Auriemma, F.; De Rosa, C.; Corradini, P. Following article in this issue.